discussion, we may conclude that ligand cyclization makes impossible the rotation of the uncoordinated amine group of the reaction intermediates from the vicinity of the metal ion, resulting in the retardation of the protonation of the uncoordinated amine group, the retardation of the breakage of the copper–nitrogen bond, the acceleration of the deprotonation of the uncoordinated amine group, and the acceleration of the formation of the copper–nitrogen bond. These effects can throw light on the kinetic and thermodynamic properties of macrocyclic compounds.

In the isomerization reaction (eq 2), crystal structure determinations of the reactant and the product indicate that one of the four nitrogens must be inverted during this reaction. In strongly acidic media, this reaction is acid catalyzed due to the required cleavage of one copper–nitrogen bond as shown in Figure 4. It is most interesting that this blue-to-red interconversion in basic solution is base catalyzed.[5] In contrast to the isomerization in acidic media, the base-catalyzed configurational conversion occurs while the ligand is coordinated, and a concerted mechanism is proposed for the reaction of coordinated hydroxide ion with amine hydrogens.[5,13]

Acknowledgment. This work was supported by a grant from the Chemistry Research Center, National Science Council of the Republic of China, to which the authors wish to express their thanks.

Registry No. [Cu(tet a)(blue)]$^{2+}$, 73464-68-3; [Cu(tet a)(red)]$^{2+}$, 73464-69-4.

---

(13) Liang, B.-F.; Margerum, D. W.; Chung, C.-S. *Inorg. Chem.* **1979**, *18*, 2001.

Contribution from the School of Chemistry,
The University of New South Wales, Kensington, New South Wales 2033, Australia

The Zinc–Benzenethiolate–Halide System. Synthesis and Structure of the Hexakis(μ-(benzenethiolato))-bis(benzenethiolato)dichlorotetrazincate(II) Dianion

IAN G. DANCE

Received July 1, 1980

The crystallization of complexes $(Me_4N)_2[Zn_4(SPh)_8X_2]$ (X = Cl, Br), $(Me_4N)_2[Zn_4(SPh)_9Cl]$, and $(Me_4N)_2[Zn_4(SPh)_{10}]$ from alcohol–acetone solutions containing solvated zinc(II), benzenethiolate, and halide ions is described and interpreted in terms of equilibria involving these and other species. The adamantane cage structure of $[(\mu\text{-}SPh)_6(ZnSPh)_4]^{2-}$ occurs also in $[(\mu\text{-}SPh)_6(ZnSPh)_2(ZnX)_2]^{2-}$ (X = Cl, Br (isostructural)) with two terminal halide ligands. No evidence for halide substitution of more than two terminal positions has been obtained. Slight distortions of the adamantane cage, principally in the positions of the bridging sulfur atoms, are associated with differentiated phenyl ring orientations, not the chloride substitution which has no detectable influence on the geometry of the cage. Mean distances are $Zn\text{–}S(Cl)_{terminal} = 2.257 \pm 0.007$ and $Zn\text{–}S_{bridging} = 2.358 \pm 0.005$ Å. Crystal data: $a = 12.377$ (2) Å, $b = 16.592$ (3) Å, $c = 16.967$ (3) Å, $\alpha = 76.68$ (1)°, $\beta = 69.92$ (1)°, $\gamma = 72.57$ (1)°, $P\bar{1}$, $Z = 2$, 4138 observed reflections, $R = 0.052$.

Introduction

Exploratory research on the coordination chemistry intrinsic to the fundamental thiolate donor function RS^-, as manifest in homoleptic metal thiolate complexes $[M_x(SR)_y]$ and complexes in which thiolate ligands predominate, has revealed new patterns of complex formation and structure. General results relevant to the observations described in this paper include the following: (i) monometallic complexes $[M(SR)_4]^{2-}$ and tetrametallic complexes $[M_4(SR)_{10}]^{2-}$, both with tetrahedral metal coordination, exist in solution equilibria and can be isolated;[1-5] (ii) the adamantane cage structure $[(\mu\text{-}SR)_6(MSR)_4]$ is ubiquitous;[1-5] (iii) solvent coordination is significant only in systems with $Zn(SPh)_2$ stoichiometry, and there exist solvent dependent reactions interconverting structurally molecular and structurally nonmolecular compounds;[2] (iv) halide coordination appears not to be competitive with benzenethiolate coordination in complexes of Cu(I), Ag(I), Sn(IV), or Pb(II),[6-9] but mixed pentafluorobenzenethiolate–chloride complexes are known;[10] (v) an internal spherical halide ligand can provide structural stability for a large cage;[11] (vi) despite the pseudohalide characteristics of the thiolate function, the formulations and structures of homoleptic metal thiolate cage complexes have no precedent in metal halide complexes.

A question that arises from these generalizations is whether terminal ligand positions on the adamantane cage structure can be substituted by halide (X), or by solvent or other uncharged ligands (L), in complexes $[(\mu\text{-}SR)_6(MSR)_{4-n}(MX)_n]^{2-}$ or $[(\mu\text{-}SR)_6(MSR)_{4-n}(ML)_n]^{n-2}$ (n = 1–4). This paper describes the crystallization of adamantane cage complexes from solutions containing Zn^{2+}, PhS^-, and Cl^- or Br^-. Conditions for crystallization of the disubstituted cage $[(\mu\text{-}SPh)_6(ZnSPh)_2(ZnX)_2]^{2-}$ (X = Cl, Br) with Me_4N^+ have been defined, and the structure of this cage has been determined by diffraction analysis. Solutions of this type crystallize also the unsubstituted cage, in $(Me_4N)_2[(\mu\text{-}SPh)_6(ZnSPh)_4]$, and a compound which probably contains the monosubstituted

---

(1) Dance, I. G. *J. Am. Chem. Soc.* **1979**, *101*, 6264.
(2) Dance, I. G. *J. Am. Chem. Soc.* **1980**, *102*, 3445.
(3) Swenson, D; Baenziger, N. C; Coucouvanis, D. *J. Am. Chem. Soc.* **1978**, *100*, 1932. Coucouvanis, D., private communication, 1980.
(4) Dance, I. G.; Guerney, P. J.; Zimmermann, W., unpublished work on $[Cd(SPh)_4]^{2-}$ and $[Cd_4(SPh)_{10}]^{2-}$.
(5) Hagen, K. S.; Berg, J. M.; Holm, R. H. *Inorg. Chim. Acta* **1980**, *45*, L17.
(6) Halide ligands are not present in complexes crystallized from a variety of solutions containing both halide and benzenethiolate.[7-9]
(7) Dance, I. G.; Calabrese, J. C. *Inorg. Chim. Acta* **1976**, *19*, L41.
(8) Dance, I. G. *Aust. J. Chem.* **1978**, *31*, 2195.
(9) Dance, I. G.; Katende, S.; Calabrese, J. C., to be published.
(10) Muller, M.; Clark, R. J. H.; Nyholm, R. S. *Transition Met. Chem.* **1978**, *3*, 369.
(11) Dance, I. G. *J. Chem. Soc., Chem. Commun.* **1980**, 818.

0020-1669/81/1320-2155$01.25/0

cage, $(Me_4N)_2[(\mu\text{-}SPh)_6(ZnSPh)_3(ZnCl)]$. Attempts to crystallize tri- or tetrasubstituted adamantane cages in the zinc–benzenethiolate–halide system have not been successful.

Experimental Section

Benzenethiol and the amines were commercial products (>97%) and were stored in contact with molecular sieves. Tetramethylammonium chloride and bromide were dried with P_4O_{10}. Fresh samples of hexahydrated zinc nitrate and anhydrous zinc chloride were used. The solvents had not been dried. All preparative solutions were deoxygenated with a dinitrogen flush and stored under an atmosphere of dinitrogen.

Bis(tetramethylammonium) Hexakis(μ-benzenethiolato))-bis(benzenethiolato)dichlorotetrazincate(II), $(Me_4N)_2[(\mu\text{-}SPh)_6(ZnSPh)_2(ZnCl)_2]$. To a stirred solution containing benzenethiol (4.4 g, 40 mmol), triethylamine (4.0 g, 40 mmol), and tetramethylammonium chloride (2.0 g, 1.8 mmol) in methanol (100 mL) at room temperature was added slowly a solution of $Zn(NO_3)_2{\cdot}6H_2O$ (6.0 g, 20 mmol) in methanol (60 mL). During this addition a white precipitate which formed was redissolved by addition of minimum volumes of acetone: a total of 35 mL of acetone was required. The flask containing this solution was sealed and allowed to stand undisturbed at 20 °C for 10 days. Crystallization commenced within 1 h. The product was filtered, washed with methanol, and vacuum-dried. The yield was 6.15 g (90%).

Analogous experiments using (i) morpholine (3.5 g) in place of triethylamine, with total solvent composition 150 mL methanol plus 20 mL acetonitrile and crystallization at 0 °C, or (ii) *N*-methylmorpholine (4.0 g) with total solvent composition 165 mL plus 45 mL acetone and crystallization at 20 °C gave the same crystalline product in similar yield. Anal. Calcd for $C_{56}H_{64}N_2S_8Cl_2Zn_4$: C, 49.67; H, 4.76; N, 2.07; S, 18.94. Found: C, 49.85; H, 4.68; N, 1.93; S, 18.81. Calcd for $C_{56}H_{65}N_2S_8O_{0.5}Cl_2Zn_4$ (see Crystallography): C, 49.35; H, 4.81; N, 2.06; S, 18.82.

$(Me_4N)_2[(\mu\text{-}SPh)_6(ZnSPh)_2(ZnCl)_2]$ is readily soluble in acetonitrile and slightly soluble in acetone at 20 °C, but neither dissolves in nor immediately reacts with water at 20 °C. The crystals give no indication of decomposition in air at 20 °C during 10 days.

The crystals used for the diffraction experiments were obtained from a preparative mixture with a different metal–ligand proportion. To a stirred solution containing benzenethiol (6.6 g, 60 mmol), tripropylamine (8.4 g, 59 mmol), tetramethylammonium chloride (2.7 g, 25 mmol) in methanol (220 mL) and acetonitrile (50 mL), at 20 °C, was added a solution of $ZnCl_2$ (5.4 g, 40 mmol). The solution was allowed to stand undisturbed for 5 days, while the product crystallized as clumps of columnar needles. The crystals were filtered, washed with methanol and ethanol, and vacuum-dried.

Bis(tetramethylammonium) Hexakis(μ-(benzenethiolato))-bis(benzenethiolato)dibromotetrazincate(II), $(Me_4N)_2[(\mu\text{-}SPh)_6(ZnSPh)_2(ZnBr)_2]$. A crystallization solution was prepared in the same manner as that for the chloride homologue above, except that tetramethylammonium bromide (2.75 g, 18 mmol) was used and the total solvent composition was 150 mL methanol and 50 mL acetone. Crystallization occurred during 3 days at room temperature, as clumps of microcrystals, which were filtered, washed with methanol, and vacuum-dried. The powder diffraction pattern confirmed that the structure and composition of this product are the same as those of the chloride homologue: *d* spacings in Å (values for $(Me_4N)_2[(\mu\text{-}SPh)_6(ZnSPh)_2(ZnCl)_2]$ in parentheses) are 15.63 w (15.51 m), 12.04 s (11.95 s), 10.76 vs (10.79 s), 10.43 s (10.35 s), 8.33 vw (8.28 m), 8.10 m (8.10 vw), 7.89 m (7.88 m, 7.81 m), 7.62 m (7.58 m), 7.47 w (7.51 vw, 5.99 vw), 5.48 w (5.41 w), 5.37 w (5.32 vw, 5.22 w), 4.72 w (4.66 m), 4.59 vw (4.58 w), 4.14 w (4.14 m), 4.04 m (4.07 s, 4.01 w), 3.94 m (3.92 m), and 3.80 m (3.82 m, 3.73 w).

Attempts to prepare $(Et_4N)_2[(\mu\text{-}SPh)_6(ZnSPh)_2(ZnX)_2]$ (X = Cl, Br) with mixtures analogous to those described above have yielded only oils.

Attempts to prepare $(R_4N)_2[(\mu\text{-}SPh)_6(ZnX)_4]$ (X = Cl, Br) have not been successful. Solutions containing PhS^-/Zn^{2+} molar ratios of 1.5 or less and varying excesses of Cl^- have yielded mixtures of $(Me_4N)_2[(\mu\text{-}SPh)_6(ZnSPh)_2(ZnCl)_2]$ and $(Me_4N)_2ZnCl_4$. For instance, a solution was prepared containing benzenethiol (3.3 g, 30 mmol), tripropylamine (4.3 g, 30 mmol), tetramethylammonium chloride (1.8 g, 16 mmol), and anhydrous zinc chloride (3.0 g, 22 mmol) in methanol (100 mL) and acetone (50 mL), at 20 °C. A fine precipitate that appeared soon after mixing could be dissolved by heating the solution (sealed) to 60 °C. Slow cooling caused large needles of $(Me_4N)_2ZnCl_4$ (identified by X-ray diffraction) to grow, followed by crystals of $(Me_4N)_2[(\mu\text{-}SPh)_6(ZnSPh)_2(ZnCl)_2]$. Increase in the proportion of the aprotic solvent in solutions of this type generally increases the yield of $(Me_4N)_2ZnCl_4$.

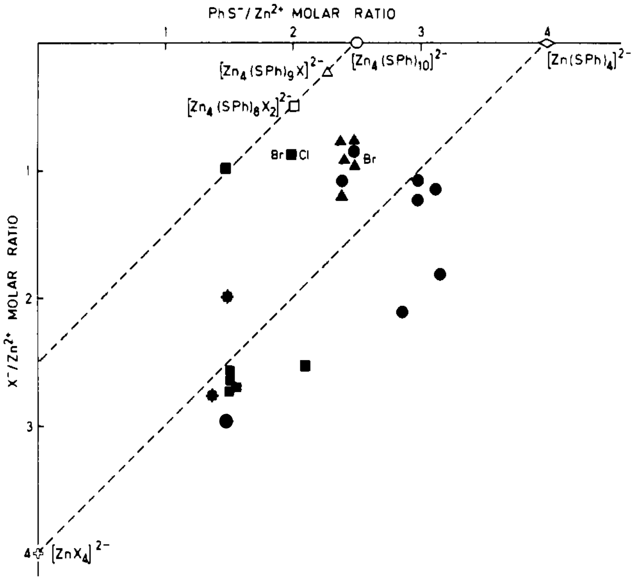

Figure 1. Products crystallizing in the Zn–PhS–Cl(Br) system, plotted in terms of the PhS^-/Zn^{2+} molar ratios in crystallization solutions. Open symbols show the stoichiometries of anionic complexes which can be isolated. The corresponding filled symbols locate the solution compositions which yielded those anions, crystallized with Me_4N^+. The dotted lines indicate ligand/Zn^{2+} ratios of 10/4 and 4/1. Results for $PhS^-/Zn^{2+} > 4$ are not included on this diagram. X is Cl except where labeled Br.

A comparison of product composition with solution composition for this and more than 20 other experiments in the Zn^{2+}–PhS^-–X^- system is given in Figure 1. All experiments involved mixtures of alcohols and aprotic solvents: minor changes in solvent ratios did not affect the product composition but did influence the quality of the crystals obtained.

Bis(tetramethylammonium) Hexakis(μ-(benzenethiolato))-tris(benzenethiolato)chlorotetrazincate(II), $(Me_4N)_2[(\mu\text{-}SPh)_6(ZnSPh)_3(ZnCl)]$. A solution containing benzenethiol (4.4 g, 40 mmol), tripropylamine (5.6 g, 39 mmol), and tetramethylammonium chloride (1.66 g, 15 mmol) in methanol (80 mL) was prepared at 20 °C, and to it was added a solution of $Zn(NO_3)_2{\cdot}6H_2O$ (5.0 g, 17 mmol) in methanol (50 mL) together with acetone (30 mL) to dissolve the initial precipitation. This solution was allowed to stand in a sealed flask at 20 °C for 10 days. A small amount of very viscous oil formed first, but this soon crystallized, and clumpy crystallization continued slowly along the walls of the flask. The product (4.3 g) was collected, washed with methanol, and vacuum-dried. Anal. Calcd for $C_{62}H_{69}N_2ClS_9Zn_4$: C, 52.16; H, 4.87; N, 1.96; S, 20.21. Found: C, 51.91, 51.70; H, 4.63, 4.75; N, 1.83, 1.88; S, 19.73, 19.15. Polycrystalline diffraction pattern spacings (Å) are 16.70 m, 11.65 s, 11.45 s, 10.90 s, 10.76 m, 8.43 w, 8.29 wm, 8.124 vw, 9.913 m, 7.678 w, 7.483 vw, 7.147 w, 6.755 w, 6.468 vw, 6.053 vw, 5.467 m, 4.824 vw, 4.649 vw, 4.440 m, 4.291 m, 4.208 ms, 4.139 w, 3.967 s, 3.952 ms, 3.809 m, 3.755 m, 3.630 w, 3.280 m, 3.000 w, and 2.954 w. Crystals suitable for diffraction analysis have not yet been obtained.

Crystallography. After preliminary photographs all crystallographic data was obtained with a Siemens diffractometer. Details are presented in Table I. As expected from the softness of the crystals, high-angle diffraction data could not be observed. Corrections were applied for the intensity loss due to radiation damage and for absorption, as previously described.[12]

Structure solution was effected by direct methods (MULTAN) and completed by least-squares plus Fourier methods. Phenyl ring hydrogen atoms were included at calculated positions. After anisotropic

---

[12] Boyd, I. W.; Dance, I. G.; Landers, A. E.; Wedd, A. G. *Inorg. Chem.* **1979**, *18*, 1875.

Table I. Crystallographic Details for $(Me_4N)_2[(\mu\text{-}SPh)_6(ZnSPh)_2(ZnCl)_2]$

habit	colorless prisms
faces	{111}, {010}, (101), $(\bar{1}\bar{1}0)$
max dimens, mm	0.2
space group	$P\bar{1}$
a, Å	12.377 (2)
b, Å	16.592 (3)
c, Å	16.967 (3)
α, deg	76.68 (1)
β, deg	69.92 (1)
γ, deg	72.57 (1)
V, Å^3	3090.6
T, °C	22
Z	2
compn of asymmetric unit	$Zn_4S_8Cl_2N_2C_{56}H_{64}$ + $(OH_2)_{0.36}$
d_{obsd}, g cm^{-3}	1.44 (2)
d_{calcd}, g cm^{-3}	1.46
radiatn	Cu Kα
μ, cm^{-1}	53.9
min and max values of transmission factor	0.34, 0.61
$2\theta_{max}$, deg	100
no. of intens measurements	6369
decay of std intens	1–0.75
criterion for obsd reflctn	$I/\sigma(I) > 2.58$
no. of independent data, m	4138
no. of variables refined, n	653
limitation, no. of data in final refinement	$(\sin\theta)/\lambda > 0.1$, 4084
$R = \Sigma^m\lvert\Delta F\rvert/\Sigma^m\lvert F_o\rvert$	0.052
$R_w = [\Sigma^m w\lvert\Delta F\rvert^2/\Sigma^m w\lvert F_o\rvert^2]^{1/2}$	0.061
$[\Sigma^m\lvert\Delta F\rvert^2/(m-n)]^{1/2}$	1.96

refinement of all nonhydrogen atoms of the 112 atom model $(C_4N)_2Zn_4(SC_6H_5)_8Cl_2$, the residual R was 0.056 for 4084 observed reflections with $(\sin\theta)/\lambda > 0.1$. At this stage a difference synthesis contained a peak of 1.1 e Å^{-3} in an empty region in the vicinity of the terminally bound thiolate sulfur atom S4. It was apparent that some scattering material was present, and since the volume of the hole it occupied was approximately that of a water molecule, the scatterer was included in further refinement as a variable fraction of an oxygen atom, with isotropic vibration (B = 15 Å^2) slightly larger than that of surrounding atoms. Refinement converged (R_w, 0.065→0.061) with oxygen at occupancy 0.36. The diffraction data were not of sufficient quality for further modeling of the cell contents: the crystal decay during irradiation may have been related to partial loss of solvent. The largest positive peaks (<0.53 e Å^{-3}) in the final difference map had no chemical significance.

The atom labeling scheme (see Figure 2) is as follows: Znp (p = 1–4); bridging benzenethiolate sulfur Spq bridging Znp, Znq; Clr terminally bound to Znr (r = 1, 2); terminal benzenethiolate sulfur Sr bound to Znr (r = 3, 4). Phenyl ring atoms on sulfur Sx are Cxy (y = 1–6); the ring hydrogen atom on Cxy is HCxy; the cation atoms are Nn and CmNn, (n = 1, 2; m = 1–4).

Neutral-atom scattering factors and anomalous dispersion corrections for zinc, sulfur, and chlorine were those of ref 13. Final coordinates and their estimated standard deviations are set out in Table II for the nonhydrogen atoms. Average values of the minimum and maximum root mean square displacement are 0.23 and 0.31 Å for the zinc atoms, 0.24 and 0.35 Å for the sulfur and chlorine atoms, 0.28 and 0.45 Å for the ring carbon atoms, and 0.31 and 0.66 Å for the cation atoms. A complete tabulation of atomic parameters and a listing of observed and calculated structure factors are included as supplementary material.

Results

Synthesis. It is apparent that many zinc–benzenethiolate complexes are present in deoxygenated solutions prepared from solvated zinc(II), benzenethiol (plus equimolar amine), and chloride or bromide ion, in solvent mixtures containing mainly the lower alcohols. Oils are often obtained, and crystalline products have been isolated in reproducible procedures only when Me_4N^+ is present. The crystalline compounds prepared by this method are $(Me_4N)_2[Zn(SPh)_4]$ (in two crystal forms), $(Me_4N)_2[Zn_4(SPh)_{10}]$, $(Me_4N)_2[Zn_4(SPh)_8X_2]$ (X = Cl, Br), $(Me_4N)_2[Zn_4(SPh)_9Cl]$, and (cation)$[ClZn_8(SPh)_{16}]$. The identity of the cation in the last compound is uncertain.[11] Details of the syntheses and structures of the two crystals containing $[Zn(SPh)_4]^{2-}$ will be published separately. Determination of the crystal structure of $(Me_4N)_2[Zn_4(SPh)_8Cl_2]$ (with which the bromo analogue is isostructural) confirms the occurrence of the disubstituted adamantane cage anion $[(\mu\text{-}SPh)_6(ZnSPh)_2(ZnX)_2]^{2-}$ shown in Figures 2 and 3.

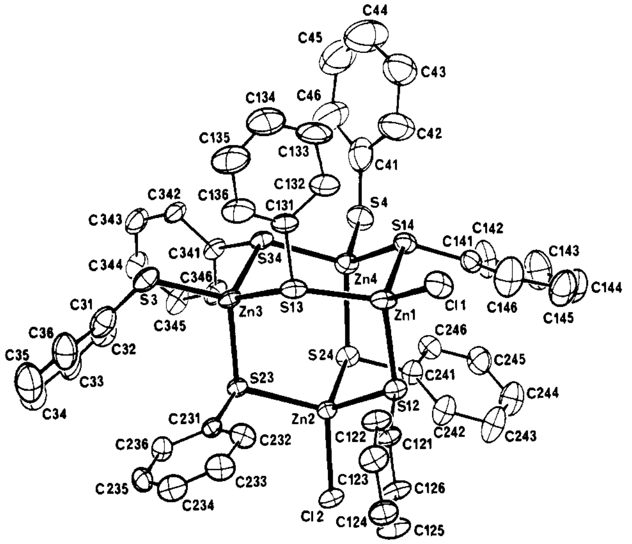

Figure 2. $[(\mu\text{-}SPh)_6(ZnSPh)_2(ZnCl)_2]^{2-}$ molecular cage. Thermal ellipsoids represent 15% probability.

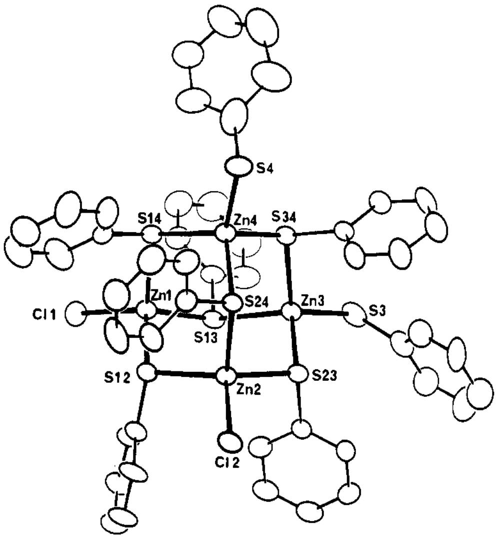

Figure 3. $[(\mu\text{-}SPh)_6(ZnSPh)_2(ZnCl)_2]^{2-}$ molecular cage, showing the differentiated orientations of phenyl rings.

In the zinc–benzenethiolate system there is no charge-transfer absorption much lower in energy than intraligand absorption. Therefore, in the absence of a convenient spectroscopic probe, crystallization and subsequent analysis by diffraction have been employed to explore the formation of complexes in solution. It is recognized that product crystallization is controlled by solubility and possibly the vagaries of nucleation, in addition to equilibrium concentrations in solution. Nevertheless the crystallization results, which are set out in Figure 1 as product composition in terms of solution composition, are self-consistent.

---

(13) "International Tables for X-ray Crystallography"; Kynoch Press: Birmingham, England, 1974; Vol. IV, Tables 2.2A and 2.3.1.

Table II. Nonhydrogen Atom Coordinates for $(Me_4N)_2[(\mu\text{-SPh})_6(ZnSPh)_2(ZnCl)_2]$

atom	*x*	*y*	*z*	atom	*x*	*y*	*z*
Zn1	0.7071 (1)	0.7033 (1)	−0.0987 (1)	C141	0.8139 (9)	0.5348 (6)	−0.2055 (7)
Zn2	0.6796 (1)	0.8547 (1)	−0.3034 (1)	C142	0.8658 (14)	0.5027 (9)	−0.2764 (9)
Zn3	0.8852 (1)	0.8844 (1)	−0.1905 (1)	C143	0.8248 (18)	0.4423 (10)	−0.2972 (10)
Zn4	0.9715 (1)	0.6807 (1)	−0.3043 (1)	C144	0.7280 (15)	0.4208 (11)	−0.2476 (14)
Cl1	0.6054 (2)	0.6361 (2)	0.0230 (2)	C145	0.6748 (13)	0.4481 (12)	−0.1778 (14)
Cl2	0.5546 (2)	0.9268 (2)	−0.3790 (2)	C146	0.7164 (13)	0.5092 (12)	−0.1549 (11)
S3	0.9536 (2)	0.9779 (2)	−0.1541 (2)	C231	0.6604 (7)	1.0316 (6)	−0.2283 (5)
S4	1.1290 (3)	0.6024 (2)	−0.3943 (2)	C232	0.5685 (9)	1.0119 (7)	−0.1588 (6)
S12	0.5853 (2)	0.7648 (2)	−0.1870 (1)	C233	0.4854 (9)	1.0784 (8)	−0.1167 (6)
S13	0.7668 (2)	0.8116 (2)	−0.0693 (1)	C234	0.4947 (10)	1.1581 (8)	−0.1419 (7)
S14	0.8723 (2)	0.6062 (2)	−0.1752 (2)	C235	0.5844 (10)	1.1771 (6)	−0.2081 (8)
S23	0.7717 (2)	0.9496 (2)	−0.2841 (1)	C236	0.6699 (9)	1.1133 (7)	−0.2525 (6)
S24	0.8416 (2)	0.7609 (2)	−0.3848 (1)	C241	0.7924 (9)	0.6903 (6)	−0.4173 (6)
S34	1.0371 (2)	0.7732 (2)	−0.2554 (1)	C242	0.6740 (10)	0.6914 (8)	−0.3949 (7)
C31	0.9559 (10)	1.0632 (9)	−0.2332 (8)	C243	0.6360 (12)	0.6372 (10)	−0.4245 (9)
C32	1.0048 (11)	1.0587 (9)	−0.3207 (8)	C244	0.7190 (15)	0.5796 (10)	−0.4777 (9)
C33	1.0092 (14)	1.1232 (11)	−0.3795 (9)	C245	0.8374 (13)	0.5792 (8)	−0.5009 (8)
C34	0.9567 (16)	1.2050 (12)	−0.3602 (13)	C246	0.8747 (10)	0.6335 (7)	−0.4718 (7)
C35	0.9146 (20)	1.2122 (13)	−0.2769 (17)	C341	1.1234 (8)	0.8288 (6)	−0.3463 (5)
C36	0.9078 (14)	1.1442 (12)	−0.2155 (10)	C342	1.2249 (9)	0.8427 (7)	−0.3457 (7)
C41	1.2210 (20)	0.5457 (12)	−0.3473 (10)	C343	1.2881 (10)	0.8896 (9)	−0.4152 (9)
C42	1.2024 (16)	0.4833 (13)	−0.2779 (14)	C344	1.2514 (11)	0.9229 (8)	−0.4861 (7)
C43	1.2894 (20)	0.4260 (13)	−0.2408 (14)	C345	1.1525 (10)	0.9067 (8)	−0.4869 (6)
C44	1.4037 (21)	0.4310 (19)	−0.2688 (18)	C346	1.0889 (9)	0.8596 (7)	−0.4180 (6)
C45	1.4431 (22)	0.4730 (20)	−0.3480 (20)	N1	0.3238 (9)	0.1633 (7)	0.6546 (6)
C46	1.3546 (22)	0.5384 (17)	−0.3868 (19)	C1N1	0.2361 (16)	0.2488 (10)	0.6628 (12)
C121	0.4472 (7)	0.8311 (6)	−0.1321 (6)	C2N1	0.3270 (21)	0.1267 (13)	0.5805 (12)
C122	0.4230 (8)	0.8430 (7)	−0.0491 (6)	C3N1	0.4455 (15)	0.1777 (15)	0.6310 (19)
C123	0.3131 (9)	0.8914 (8)	−0.0089 (6)	C4N1	0.2989 (19)	0.0951 (13)	0.7317 (10)
C124	0.2292 (9)	0.9269 (8)	−0.0500 (8)	N2	0.2822 (13)	0.6342 (9)	0.8921 (10)
C125	0.2561 (9)	0.9167 (9)	−0.1319 (8)	C1N2	0.1976 (17)	0.7249 (11)	0.9133 (12)
C126	0.3640 (8)	0.8700 (8)	−0.1738 (6)	C2N2	0.2075 (15)	0.5680 (11)	0.8988 (17)
C131	0.8537 (8)	0.7676 (7)	0.0006 (6)	C3N2	0.3517 (17)	0.6372 (21)	0.7966 (17)
C132	0.8855 (11)	0.6813 (9)	0.0271 (8)	C4N2	0.3629 (22)	0.6116 (14)	0.9497 (18)
C133	0.9517 (14)	0.6526 (11)	0.0888 (11)				
C134	0.9889 (17)	0.7068 (15)	0.1154 (11)				
C135	0.9505 (15)	0.7862 (13)	0.0912 (10)	O	1.3173 (26)	0.6996 (19)	−0.5579 (19)
C136	0.8845 (12)	0.8195 (9)	0.0350 (8)				

Attention should be drawn to the following points about the results in Figure 1. (a) All tetrazinc cage compounds crystallize from solutions containing ligands in excess of the stoichiometric ligand/zinc ratio of 10/4. For example, $[Zn_4(SPh)_{10}]^{2-}(Me_4N^+)$ crystallizes from solutions containing Cl/Zn $\simeq$ 2 and PhS/Zn $\simeq$ 3, sufficient for the formation of $[Zn(SPh)_3Cl]^{2-}$ or $[Zn(SPh)_2Cl_2]^{2-}$. No evidence has appeared yet for crystallization of the mixed-ligand complexes $[Zn(SPh)_{4-n}Cl_n]^{2-}$ (n = 1–3). (b) The production of $[Zn_4(SPh)_8Cl_2]^{2-}(Me_4N^+)$ from solutions with excess chloride (Cl/Zn $\simeq$ 2.7) and deficient in benzenethiolate (PhS/Zn $\simeq$ 1.5) implies that Cl^- competes poorly with PhS^- as a terminal ligand on Zn. (c) Mixtures with the stoichiometry of $[Zn_4(SPh)_6Cl_4]^{2-}$ yielded only $[Zn_4(SPh)_8Cl_2]^{2-}$, and increases in the Cl/Zn ratio in attempt to force the formation of $[Zn_4(SPh)_6Cl_4]^{2-}$ led only to the crystallization of $[ZnCl_4]^{2-}$. $(Me_4N)_2ZnCl_4$ has limited solubility in the solvent systems employed. There is no evidence for crystallization of the mixed-ligand complexes $[Zn_4(SPh)_{10-n}Cl_n]^{2-}$ (n = 3, 4): on the basis of products crystallizing it appears that they are disproportionating to $[Zn_4(SPh)_8Cl_2]^{2-}$.

Molecular Structure of $[(\mu\text{-SPh})_6(ZnSPh)_2(ZnCl)_2]^{2-}$. The structural results are presented in Figures 2 and 3, with dimensions tabulated in Table III. The crystals contain isolated molecular cages, $[(\mu\text{-SPh})_6(ZnSPh)_2(ZnCl)_2]^{2-}$, with no unusual intercage contacts: the shortest intercage distance is HC36–HC135 ($2-x$, $2-y$, $-z$) at 2.40 Å. There is evidence for partial occupation of a hole in the crystal by solvent, probably water, which is weakly hydrogen bonded to S4. The pertinent distances are given in Table III.

Chemically comparable dimensions of the cluster are assembled in the following statistical summary, expressed as dimension, sample size, mean value of the dimension, and estimated standard deviation of the mean value: Zn–S-$(Cl)_{terminal}$, 4, 2.257, 0.014, 0.007 Å; Zn–$S_{bridging}$, 12, 2.358, 0.016, 0.005 Å; Cl–Zn–$S_{bridging}$, 6, 109.9, 0.9, 0.4°; $S_{terminal}$–Zn–$S_{bridging}$, 6, 111.8, 3.8, 1.6°; $S_{bridging}$–Zn–$S_{bridging}$, 12, 108.0, 5.3, 1.5°; Zn–$S_{bridging}$–Zn, 6, 111.7, 2.3, 0.9°; S–C, 8, 1.74, 0.08, 0.03 Å; Zn–S–C, 14, 107.4, 2.6, 0.7°; N–C, 8, 1.54, 0.04, 0.01 Å; Zn–Zn, 6, 3.90, 0.05, 0.02 Å; $S_{bridging}$–$S_{bridging}$, 12, 3.81, 0.12 , 0.04 Å. All bond lengths are normal. Any difference between the terminal bonds Zn–SPh and Zn–Cl is marginal. The lengthening of Zn–$S_{bridging}$ over Zn–$S_{terminal}$ is 0.10 Å.

In the idealized (point group T_d) adamantane cage all angles at bridging sulfur and at zinc are tetrahedral, and the Zn–Zn and S–S distances are equal. The $[(\mu\text{-SPh})_6(ZnSPh)_2(ZnCl)_2]^{2-}$ cage, which possesses no crystallographic symmetry, displays small systematic deviations and some larger nonsystematic deviations from this ideal. There is slight extension of the zinc atoms out along the threefold axes of the cage, revealed by $S_{bridging}$–Zn–$S_{bridging}$ < 109.5° < Zn–$S_{bridging}$–Zn and $S_{bridging}$–$S_{bridging}$ (3.81 Å) < Zn–Zn (3.90 Å). The latter two dimensions are 3.82 and 3.83 Å, respectively, in *catena*-$(\mu\text{-SPh})[(\mu\text{-SPh})_6Zn_4(CH_3OH)(SPh)]$,[2] and 3.74 and 3.87 Å, respectively, in $[(\mu\text{-SPh})_6(CoSPh)_4]^{2-}$.[1] As in other thiolate-bridged cages the largest cage distortions occur in the positions of the bridging benzenethiolate groups and are manifest in the range of $S_{bridging}$–Zn–$S_{bridging}$ angles (101.8–121.1°) and of $S_{bridging}$–$S_{bridging}$ distances (3.65–4.09 Å: contrast the 3.84–3.97-Å range in Zn–Zn distances).

Specific distortions of S_{br}–Zn–S_{br} angles can be associated with (and possibly attributed to) the directions of the phenyl substituents of the bridging ligands. Each S_{br}–C_α vector may have two directions relative to the Zn–S_{br}–Zn plane, directions

Table III. Selected Interatomic Distances and Angles[a] in $(Me_4N)_2[(\mu\text{-SPh})_6(ZnSPh)_2(ZnCl)_2]$

	Distances		
	Zinc Coordination		
Zn1–Cl1	2.255 (3)	Zn3–S3	2.257 (3)
Zn1–S12	2.343 (3)	Zn3–S13	2.383 (3)
Zn1–S13	2.343 (3)	Zn3–S23	2.344 (3)
Zn1–S14	2.373 (3)	Zn3–S34	2.363 (3)
Zn2–Cl2	2.241 (3)	Zn4–S4	2.275 (3)
Zn2–S12	2.365 (3)	Zn4–S14	2.377 (3)
Zn2–S23	2.335 (3)	Zn4–S24	2.369 (3)
Zn2–S24	2.360 (3)	Zn4–S34	2.346 (3)
	Zn–Zn		
Zn1–Zn2	3.844 (2)	Zn2–Zn3	3.861 (2)
Zn1–Zn3	3.971 (2)	Zn2–Zn4	3.889 (2)
Zn1–Zn4	3.880 (2)	Zn3–Zn4	3.965 (2)
	$S_{bridging}$–$S_{bridging}$		
S12–S13	3.805 (4)	S24–S23	3.646 (3)
S12–S14	3.772 (4)	S23–S13	3.823 (3)
S12–S23	4.092 (3)	S34–S13	3.737 (3)
S12–S24	3.742 (3)	S34–S14	3.666 (4)
S13–S14	3.886 (4)	S34–S23	3.779 (3)
S14–S24	3.939 (4)	S34–S24	3.855 (4)
	S–C		
S3–C31	1.71 (1)	S14–C141	1.80 (1)
S4–C41	1.57 (2)[b]	S23–C231	1.79 (1)
S12–C121	1.80 (1)	S24–C241	1.73 (1)
S13–C131	1.76 (1)	S34–C341	1.78 (1)
	Distances around Solvent Location[c]		
O–HC46	2.68 (3)	O–HC236[e]	3.35 (3)
O–HC45[d]	3.01 (3)	O–S4	3.39 (3)
	Angles		
	Cl–Zn–$S_{bridging}$		
Cl1–Zn1–S12	109.5 (1)	Cl2–Zn2–S12	109.7 (1)
Cl1–Zn1–S13	109.9 (1)	Cl2–Zn2–S23	108.6 (1)
Cl1–Zn–S14	111.4 (1)	Cl2–Zn2–S24	110.2 (1)
	$S_{terminal}$–Zn–$S_{bridging}$		
S3–Zn3–S13	111.6 (1)	S4–Zn4–S14	117.4 (1)
S3–Zn3–S23	112.7 (1)	S4–Zn4–S24	106.2 (1)
S3–Zn3–S34	113.4 (1)	S4–Zn4–S34	109.2 (1)
	$S_{bridging}$–Zn–$S_{bridging}$		
S12–Zn1–S13	108.6 (1)	S13–Zn3–S23	107.9 (1)
S12–Zn1–S14	106.3 (1)	S13–Zn3–S34	103.9 (1)
S13–Zn1–S14	111.0 (1)	S23–Zn3–S34	106.8 (1)
S12–Zn2–S23	121.1 (1)	S14–Zn4–S24	112.2 (1)
S12–Zn2–S24	104.7 (1)	S14–Zn4–S34	101.8 (1)
S23–Zn2–S24	101.9 (1)	S24–Zn4–S34	109.7 (1)
	Zn–$S_{bridging}$–Zn		
Zn1–S12–Zn2	109.5 (1)	Zn2–S23–Zn3	111.2 (1)
Zn1–S13–Zn3	114.3 (1)	Zn2–S24–Zn4	110.7 (1)
Zn1–S14–Zn4	109.6 (1)	Zn3–S34–Zn4	114.7 (1)
	Zn–S–C		
Zn3–S3–C31	106.7 (4)	Zn4–S14–C141	105.6 (4)
Zn4–S4–C41	110.7 (8)	Zn2–S23–C231	108.9 (3)
Zn1–S12–C121	111.1 (3)	Zn3–S23–C231	102.6 (3)
Zn2–S12–C121	106.6 (3)	Zn2–S24–C241	110.4 (3)
Zn1–S13–C131	109.6 (4)	Zn4–S24–C241	108.2 (4)
Zn3–S13–C131	106.1 (3)	Zn3–S34–C341	103.2 (3)
Zn1–S14–C141	106.7 (3)	Zn4–S34–C341	107.0 (3)

[a] Distance in Å, angles in deg. Estimated standard deviations in parentheses refer to the least significant digit quoted. [b] This subnormal distance is regarded as an artifact of data errors caused by the crystal decay. Note that Zn–S is longer than average. [c] Probably partially occupied water location (see Experimental Section). Only distances less than 2.4 Å are listed. [d] $3-x, 1-y, -1-z$. [e] $2-x, 2-y, -1-z$.

which are axial or equatorial with respect to the $Zn_3(S_{br})_3$ chairs which constitute the adamantane cage. Each S_{br}–C_α vector belongs to two chairs, being axial to one and equatorial to the other. The largest S_{br}–Zn–S_{br} angle is S12–Zn2–S23 (121.1°), which is associated with two ligand rings which are both axial with respect to the chair which contains S12, Zn2, and S23 (see Figure 3). Thus the enlarged angle may be due to repulsions between the phenyl rings. This hypothesis is supported by further examination of the directions of the other phenyl groups. There is one other axial–axial pair of S_{br}–C_α directions, namely, ligands 14 and 24, and the S14–Zn4–S24 angle which links them is the second largest S_{br}–Zn–S_{br} angle. There are two equatorial–equatorial pairs of ligands. Bridging ligands 23 and 24 are both equatorial with respect to the Zn_3S_3 chair which links them through Zn2, and bridging ligands 14 and 34 are both equatorial with respect to the Zn_3S_3 chair involving S14, Zn4, and S34. Consistent with the absence of any phenyl ring approach in these two instances, the S23–Zn2–S24 and S14–Zn4–S34 angles are the smallest of the S_{br}–Zn–S_{br} set, namely, 101.9 and 101.8°. This differentiated orientation of phenyl groups on bridging ligands is apparent on viewing the cage about its potential threefold axes, in this case the Cl2–Zn2 and S4–Zn4 vectors. At the other two zinc atoms, Zn1 and Zn3, there is pseudothreefold symmetry of the three bridging ligand substituents around the Cl1–Zn1 and S3–Zn3 vectors, respectively. This pseudosymmetry is associated with less distortion of S_{br}–Zn–S_{br} angles, which range only from 103.9 to 110.0° at Zn1 and Zn3. The three pairs of bridging ligands which link through Zn1 and the three pairs of bridging ligands which link through Zn3 all have axial–equatorial conformations of the phenyl rings in their Zn_3S_3 chairs.

Different steric influences of Cl^- and ^-SPh as terminal ligands are not apparent.

Displacements of individual atoms from SPh ligand planes are all less than 0.04 Å, except for ligand 4 where the maximum displacement is 0.11 Å. The rotational conformation of each phenyl ring plane around the S–C_α bond is regarded[3] as significantly restricted in the tetrahedral monometallic complexes $[M(SPh)_4]^{2-}$, in that the phenyl ring plane approaches coplanarity with the Zn–S–C_α plane. In $[(\mu\text{-SPh})_6(ZnSPh)_2(ZnCl)_2]^{2-}$ the angles between the SPh ring plane of each terminal ligand (q) and the plane Znq–Sq–Cq[1] are 48.5 and 50.7° for $q = 3$ and 4. At the bridging benzenethiolate ligands the angles between the SPh ring plane of ligand pq and the Znp–Znq vector are 33, 35, 2, 74, 33, and 71° for pq = 12, 13, 14, 23, 24, and 34, respectively.

Discussion

The molecular cage $[(\mu\text{-SPh})_6(ZnSPh)_2(ZnX)_2]^{2-}$ is the second mixed halide–thiolate complex to be characterized structurally and is the first with terminal halide coordination. The present structure is the terminally disubstituted version of the antecedent adamantane molecular cage $[(\mu\text{-SPh})_6(ZnSPh)_4]^{2-}$, but there is no evidence yet from crystallization studies for tri or tetra terminally substituted adamantane cages. When crystallized with Me_4N^+ the three complexes with dihalide termination $[(\mu\text{-SPh})_6(MSPh)_2(MX)_2]^{2-}$ (M = Zn, X = Cl; M = Zn, X = Br; M = Co, X = Cl)[1] are isostructural.

No instance is known of a halide–thiolate cage with halide in the doubly bridging position which is commonly occupied by thiolate ligands. Central quadruply bridging halide occurs in the molecular cage $[ClZn_8(SPh)_{16}]^-$.[11]

Terminal coordination of methanol in place of thiolate on the adamantane cage occurs in *catena*-$(\mu\text{-SPh})[(\mu\text{-SPh})_6Zn_4(CH_3OH)(SPh)]$, which is one-dimensionally nonmolecular in structure.[2] It is possible that disolvent coordinated adamantane molecular cages, $[(\mu\text{-SPh})_6(ZnSPh)_2(Zn\text{-solvent})_2]$, uncharged analogues of the present dihalide cage, exist in alcohol and acetone solutions where the PhS/Zn ratio is 2 and halide is absent.[2]

Acknowledgment. The support of the Australian Research Grants Committee is gratefully acknowledged. D. C. Craig

assisted with collection of the diffraction data.

Registry No. $(Me_4N)_2[(\mu\text{-}SPh)_6(ZhSPh)_2(ZnCl)_2]$, 76900-55-5; $(Me_4N)_2[(\mu\text{-}SPh)_6(ZnSPh)_2(ZnBr)_2]$, 76915-19-0; $(Me_4N)_2[(\mu\text{-}SPh)_6(ZnSPh)_3(ZnCl)]$, 76900-57-7; $(Me_4N)_2[Zn_4(SPh)_{10}]$, 76915-21-4; $(Me_4N)_2[Zn(SPh)_4]$, 76915-22-5.

Supplementary Material Available: A complete tabulation of the atomic parameters and a listing of F_o and F_c (19 pages). Ordering information is given on any current masthead page.

Contribution from the Department of Inorganic Chemistry,
Charles University, 12840 Prague, Czechoslovakia

Crystal Structure of a Nickel(II) Complex of a Chiral Bis(tertiary phosphine), Bromo[(*R*,*S*)-3,6-diphenyl-3,6-diphosphaoctanedioato(1–)][(*S*,*R*)-3,6-diphenyl-3,6-diphosphaoctanedioic acid]nickel(II) Hydrate

J. PODLAHOVÁ,* B. KRATOCHVÍL, and V. LANGER[1]

Received July 21, 1980

The complex $[NiBr(HQ)(H_2Q)]\cdot H_2O$ containing the chiral bis(tertiary phosphine), $HO_2CCH_2(C_6H_5)PCH_2CH_2P(C_6H_5)CH_2CO_2H$ (H_2Q) was studied by single-crystal X-ray structural analysis. The crystal is monoclinic, $P2_1/c$, with $a = 12.155$ (2) Å, $b = 18.286$ (3) Å, $c = 17.336$ (4) Å, $\beta = 102.41$ (1)°, and $Z = 4$. The structure was determined from 3065 reflections measured on a Syntex P2$_1$ diffractometer and solved and refined by conventional Patterson, Fourier, and least-squares techniques to $R = 0.046$ and $R_w = 0.058$. All atoms except four disordered methylene hydrogens were located. The central nickel atom is five-coordinated by four phosphorus atoms forming a basal plane and bromide at the top of a tetragonal pyramid. Carboxyl groups and the water molecule are not coordinated to nickel. The stereochemistry of the complex with respect to the chiral phosphorus atoms corresponds to the anti-bis(meso-ligand) configuration. The two phosphine ligands are not equivalent: one of the chelate rings suffers from disorder of the methylene groups while the second adopts a normal λ-skew conformation. The other difference between the ligands as follows from electroneutrality demands, i.e., one being HQ^- and the other H_2Q, is rather formal because of extensive hydrogen bonding that counterbalances the differences between the carboxyls and constitutes a three-dimensional network holding the structure together.

Introduction

Complexes of chiral bis(tertiary phosphines) attract considerable interest because of their application in stereospecific homogeneous catalysis. Among many phosphine ligands, those functionalized by a second, typically hard donor group are described only rarely[2–7] despite the obvious fact that such "hybrid" ligands could exhibit properties differing significantly from those of simple phosphines. As discussed recently by Meek and co-workers,[7] the solubility of complexes, the affinity toward hard metal ions, and, hence, the catalytic activity can be expected to be influenced by the second, hard donor. A series of ligands of this type, $(C_6H_5)_{3-n}P(CH_2CO_2H)_n$ (n = 1–3), was synthesized in this laboratory[8–10] and has been proved to coordinate selectively to various metal ions. An extension of this series includes a chiral bis(tertiary phosphine) of the "hybrid" type, namely, 3,6-diphenyl-3,6-diphosphaoctanedioic acid (hereafter, H_2Q), $HO_2CCH_2(C_6H_5)PCH_2CH_2P(C_6H_5)CH_2CO_2H$, which was synthesized in small yields,[11] presumably mainly because of the isolation from a mixture of diastereoisomers. The more efficient synthesis of the same diastereoisomer (as indicated by the melting point) was described independently.[12] As the indentification of the isolated diastereoisomer by the X-ray structure determination suffered from imperfectness of the H_2Q crystals, a derivative which would crystallize well was sought to serve for this purpose. Nickel complexes synthesized and characterized previously[13] are the obvious candidates as they are prepared under mild conditions where the configuration of the ligand can safely be expected to remain unchanged.

Experimental Section

The title complex was synthesized by mixing 0.19 g of $H_2Q\cdot 0.25$(dioxane)[11] (0.5 mmol) dissolved in 5 mL of acetic acid with 0.25 mmol of $NiBr_2$ dissolved in 1 mL of water and allowing water vapor to diffuse into the solution in a closed vessel. With gradual decrease of the acetic acid concentration to ca. 30%, orange single crystals grew during several days at room temperature, yielding ca. 90% of the theoretical amount. Together with the homogeneity of the material (as proved by mp and TLC), this yield confirms that the original sample of H_2Q was not a mixture of diastereoisomers.

The IR spectrum (Nujol and Fluorolube mulls) indicated protonized and dissociated carboxyl groups in approximately a 3:1 ratio, as well as the presence of water (two small $\nu(H_2O)$ bands at 3500 and 3565 cm^{-1}). In accordance with further analytical data, the complex is best formulated as $[NiBr(HQ)(H_2Q)]\cdot H_2O$. Anal. Calcd for $C_{36}H_{41}BrNiO_9P_4$: Ni, 6.67; Br, 9.08; P, 14.07; H_2O, 2.05. Found: Ni, 6.73; Br, 9.14; P, 13.98; H_2O, 2.1 (weight loss at 170 °C under argon). The product is not identical with that obtained from aqueous acetone.[13]

Solution and Refinement of the Structure

A crystal of the title compound (dimensions 0.3 × 0.3 × 0.1 mm^3) was placed on a goniometer head in a general position. The crystal was found to be monoclinic with $a = 12.155$ (2) Å, $b = 18.286$ (3) Å, $c = 17.336$ (4) Å, $\beta = 102.41$ (1)°, and $V = 3763$ (1) Å^3. The cell dimensions were obtained by the least-squares fit of 17 reflections in the range $20° \leq 2\theta \leq 25°$, measured on a Syntex P2$_1$ automated diffractometer at room temperature with use of graphite-monochromated Mo Kα radiation ($\lambda = 0.71069$ Å). Systematic absences

---

[1] Institute of Macromolecular Chemistry, Czechoslovak Academy of Sciences, Prague.

[2] Aguiar, A. M.; Hansen, C. K.; Mague, J. T. *J. Org. Chem.* **1967**, *32*, 2383.

[3] Sacconi, L.; Gelsomini, J. *Inorg. Chem.* **1968**, *7*, 291.

[4] Meier, M. Dissertation No. 3988; Eidgenösische Technische Hochschule: Zürich, 1967.

[5] Moulton, C. J.; Shaw, B. L. *J. Chem. Soc., Dalton Trans.* **1980**, 299 and references therein.

[6] Dahl, O.; Larsen, S. *J. Chem. Res., Synop.* **1979**, 396.

[7] Uriarte, R.; Mazanec, T. J.; Tau, K. D.; Meek, D. W. *Inorg. Chem.* **1980**, *19*, 79.

[8] Jarolím, T.; Podlahová, J. *J. Inorg. Nucl. Chem.* **1976**, *38*, 125.

[9] Podlahová, J. *Collect. Czech. Chem. Commun.* **1978**, *43*, 57.

[10] Podlahová, J. *Collect. Czech. Chem. Commun.* **1978**, *43*, 3007.

[11] Ludvík, J.; Podlahová, J. *J. Inorg. Nucl. Chem.* **1978**, *40*, 967.

[12] Tzschach, A.; Friebe, S. *Z. Chem.* **1979**, *19*, 375.

[13] Ludvík, J.; Podlahová, J. *J. Inorg. Nucl. Chem.* **1978**, *40*, 1045.

0020-1669/81/1320-2160$01.25/0